NEWFIRM Discovery of Warm Molecular Hydrogen in the Wind of M82

Sylvain Veilleux (U. Maryland), David S. N. Rupke (U. Hawaii), & Rob Swaters (U. Maryland)

Galaxy-scale outflows of gas ("superwinds") are a ubiquitous phenomenon in both starburst galaxies and those containing an active galactic nucleus (Veilleux et al. 2005). The observational data set on these outflows is steadily increasing, but difficult issues remain. One vexing problem is how much different phases of the ISM contribute to the mass and energy of superwinds. Measurements have shown that winds contain cool (molecular or neutral), warm (ionized) and hot (highly ionized) material. However, the relative contribution of these phases to the total mass and energy of the wind is uncertain by an order of magnitude. The contribution from dust and molecular gas to the mass and energy in the wind is almost completely unknown. The impact of superwinds on their environments depends strongly on these quantities.

In an attempt to constrain the importance of the molecular component in winds, the NOAO Extremely Wide Field Infrared Mosaic (NEWFIRM; Probst et al. 2008 and references therein) on the Mayall 4-meter telescope at Kitt Peak was used to search for warm H_2 in the prototypical galactic wind of M82. Total on-target integrations of 40 and 420 minutes were obtained over a period of four nights in November 2008 using the broadband K_s and narrowband H_2 2.124 μm filters, respectively. The data were reduced using NOAO NEWFIRM Science Pipeline v1.0 (Swaters et al. 2009).

The continuum-subtracted H_2 image of M82 is shown in Figure 1. Immediately evident in Figure 1 are H_2 filaments extending more than $\sim$3 kpc above and below the plane of the galaxy disk, roughly coincident with the location of the galactic wind in M82. In Figures 2 and 3, our H_2 data are compared with the published Hα and 7.7 + 8.6 μm PAH images of Mutchler et al. (2007) and Engelbracht et al. (2006), respectively. The results of these comparisons favor UV excitation/heating (shock heating) as the principal H_2 emission process in the inner (outer) bright filaments of the wind, but other processes are probably at work in the fainter, more diffuse, PAH-emitting material where the H_2 emission is apparently suppressed relative to the PAHs.

The detailed processes by which the disk ISM is entrained in the wind without destroying the molecular gas and mass-loading the wind in the process are not well understood. The mere presence of molecular material $\sim$3 kpc from the disk provides strong constraints on the stability of wind-entrained clouds against photo- and thermal-evaporation, Kelvin-Helmoltz instabilities, and shedding events due to ablation. The time scale to bring such clouds out to a distance of 3 kpc is $\sim 10^7$ $(v_{\rm H2-outflow}/v_{\rm CO-outflow})^{-1}$ yrs, assuming they entered the wind near the center and the warm H_2 material shares the same kinematics as the cold molecular material ($v_{\rm CO-outflow} \sim 100$ km s^{-1}, the average deprojected outflow velocity derived from the mm-wave CO observations of Walter et al. 2002). It is not clear how these clouds can survive for this long in the wind flow.

The total amount of warm H_2 gas entrained in the wind of M82 is only $M_{H_2} \sim 1.2 \times 10^4 M_\odot$

and the total kinetic energy of this material $\sim M_{H_2} v^2_{\rm H2-outflow} \sim 10^{51}$ ergs, assuming again that the warm H_2 material shares the same kinematics as the cold molecular material. This is four orders of magnitudes lower than the kinetic energies of the entrained ionized Hα-emitting gas (Shopbell & Bland-Hawthorn 1998) and molecular CO-emitting material (Walter et al. 2002). The warm H_2 material is therefore not a dynamically important component of the outflow. However, a comparison between the H_2 emission and the distribution of the CO emission reveals that most of the features seen in CO are detected in H_2 but not the converse: as expected in photon-dominated regions (PDRs; Tielens & Hollenback 1985), the H_2 emission is more extended and probes clouds which are more diffuse (smaller A_V) and at larger distances from the nucleus than the CO emission. Deep H_2 2.12 μm observations such as these therefore represent a promising new method to study the elusive but potentially important molecular component of galactic winds.

A more detailed discussion of these results was recently published in the *Astrophysical Journal Letters* (Veilleux et al. 2009).

REFERENCES

Engelbracht, C. W., et al. 2006, ApJ, 642, L127

Lupton, R. H., Gunn, J. E., & Szalay, A. S. 1999, AJ, 118, 1406

Mutchler, M., et al. 2007, PASP, 119, 1

Probst, R. G., et al. 2008, SPIE, 7014, 93

Shopbell, P. L., & Bland-Hawthorn, J. 1998, ApJ, 493, 129

Swaters, R. A., Valdes, F., & Dickinson, M. E. 2009, preprint (astro-ph/0902.1458)

Tielens, A. G. G. M., & Hollenbach, D. 1985, ApJ, 291, 722

Veilleux, S., Cecil, G., & Bland-Hawthorn, J. 2005, ARA&A, 43, 769

Veilleux, S., Rupke, D. N. S., & Swaters, R. 2009, ApJ, 700, L149

Walter, F., Weiss, A., & Scoville, N. 2002, ApJ, 580, L21

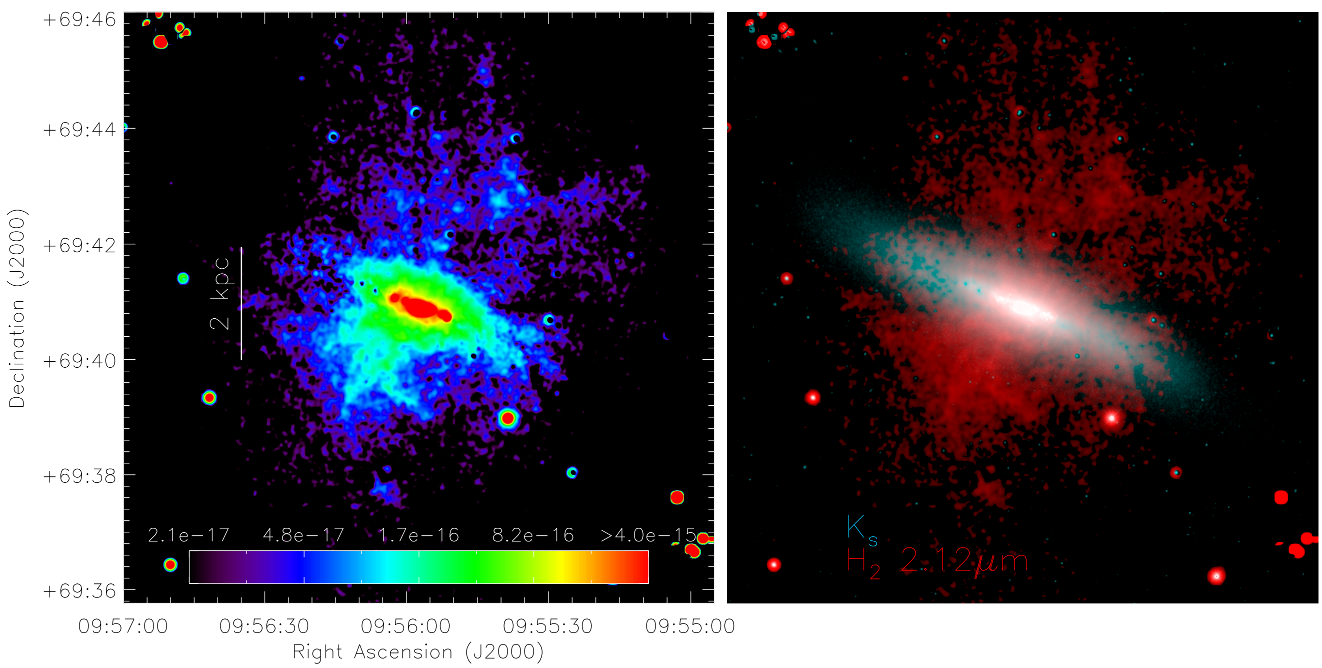

Fig. 1.— H_2 2.12 μm emission in M82. (*left*) "Pure" H_2 emission on a false-color scale. (*right*) H_2 (red) + K_s continuum (blue) emission. The H_2 data were continuum subtracted and smoothed with a 4″ Gaussian kernel to bring out the large scale structure. The intensity scalings in this figure are "asinh" from Lupton et al. (1999). The flux scale is in ergs s^{-1} cm^{-2} $arcsec^{-2}$. A distance of 3.53 Mpc for M82 was assumed.

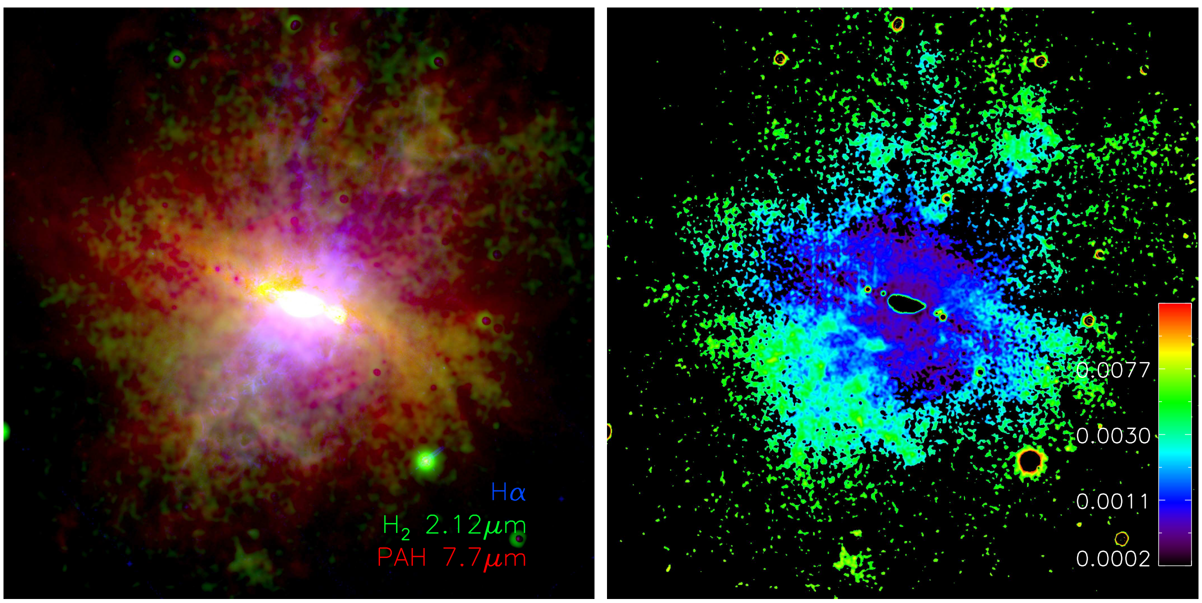

Fig. 2.— (*left*) Three-color composite of M82: *Green:* H_2 2.12 μ emission (same as Figure 1), *Red:* 7.7 + 8.6 μm PAH emission from Engelbracht et al. (2006), and *Blue: HST*/ACS continuum-subtracted Hα emission from Mutchler et al. (2007), smoothed to $0\farcs2$. See Figure 1 for information on intensity scaling. (*right*) H_2-to-PAH emisssion ratio map in the brightest H_2 filaments. Black regions are of low S/N or affected by saturation effects. The absolute ratio scale is accurate to within a factor of only $\sim$2 due to PSF mismatch between the two wavebands, lack of color corrections for the IRAC photometry, and stellar contamination to the 8 μm flux.

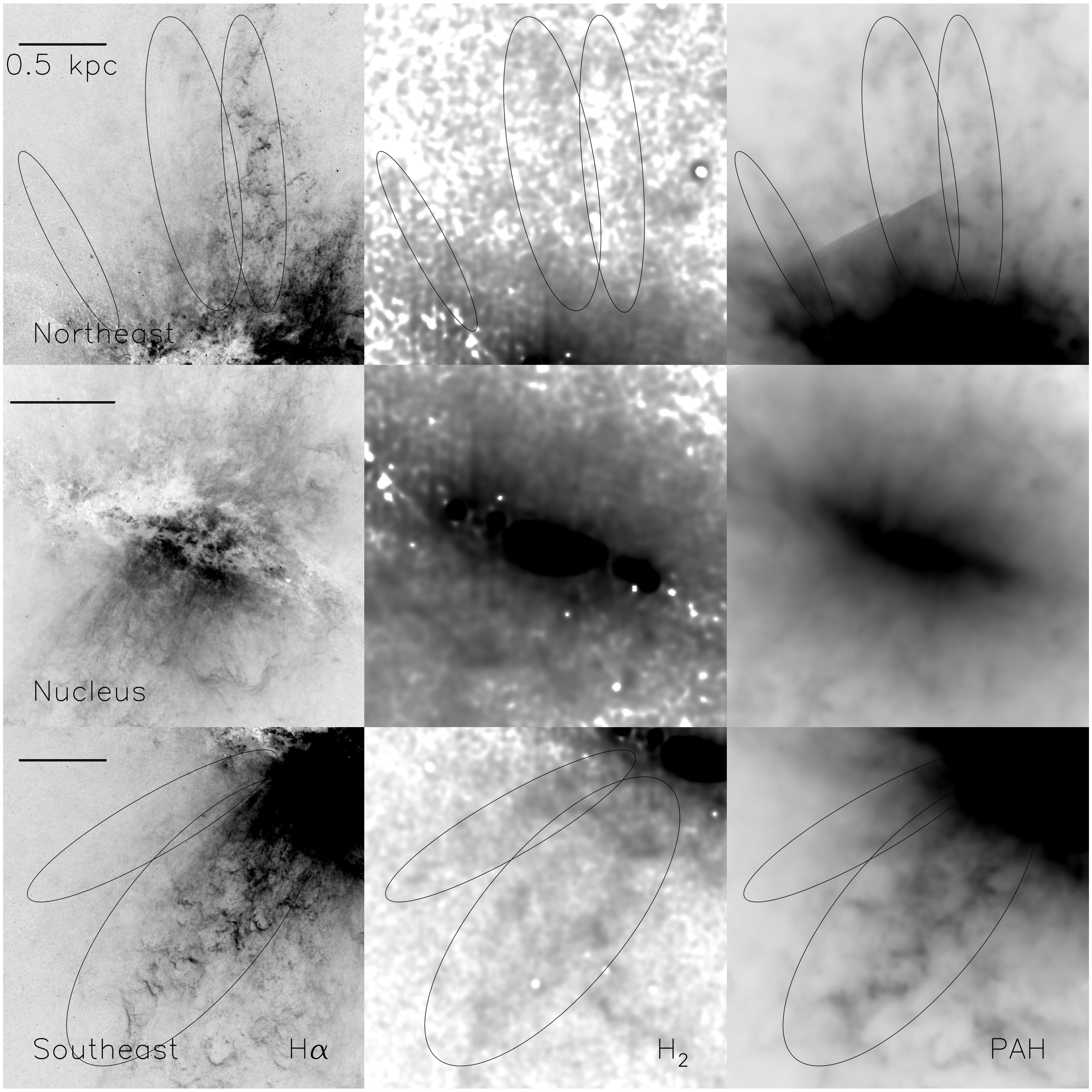

Fig. 3.— Large-scale images (2′ wide) that focus on three regions of coherent H_2 2.12 μm emission (central column; smoothed with 4″ Gaussian kernel) and compare with the Hα (left; 0.″2) and PAH (right) emission. Shown in the top, middle, and bottom rows are the NE quadrant, nuclear disk region, and SE quadrant, respectively. See Figure 1 for information on intensity scaling. The ellipses delineate prominent radial filaments that appear in at least one waveband.